Numerical Simulation of Hydraulic Jump in a Compound Channel

Samia Boudjelal
Laboratory of Applied Research in Hydraulics, Department of Hydraulic, Faculty of Technology, University of Batna 2, Batna, Algeria
s.boudjellal@univ-batna2.dz (corresponding author)

Ali Fourar
Laboratory of Applied Research in Hydraulics, Department of Hydraulic, Faculty of Technology, University of Batna 2, Batna, Algeria
a.fourar@univ-batna2.dz

Fawaz Massouh
Ecole National Supérieure d'Arts et Métiers, Paris, France
fawaz.massouh@ensam.eu

Received: 26 June 2024 | Revised: 18 July 2024, 24 July 2024, and 26 July 2024 | Accepted: 3 August 2024

 DOI: https://doi.org/10.48084/etasr.8235

ABSTRACT

This paper studies the phenomenon of hydraulic jump in compound channels using a numerical model and provides remarkable results. Several values of the opening parameter, h1, are utilized to generate the hydraulic jumps. A recirculation zone is detected by studying the RNG-K-Ɛ turbulent Volume Of Fluid (VOF) model, which is distinguished by the modified directions of the velocity vectors. When compared with the experimental values, the numerical simulation demonstrated very good accuracy, with an error of no more than 9.4%. The results underline the reliability and usefulness of the VOF turbulence model for understanding and simulating the hydraulic processes in compound channels.

Keywords-hydraulic jump; RNG-K-Ɛ turbulence model;VOF; compound channel; energy dissipation

I. INTRODUCTION

Energy dissipation in open channels is a crucial aspect of hydraulic engineering, providing a crucial mechanism for maintaining the stability and operational efficacy of water systems [1-4]. The hydraulic jump acts as a vital mechanism for energy dissipation in open channel flow, commonly observed in rivers, canals, weirs, spillways [5, 6], and floodplain systems [7]. These channels comprise a primary channel with a narrower, often deeper, secondary channel, typically separated by natural or man-made levees [8]. They are a common feature of river systems and hydraulic engineering, and their unique geometry gives rise to a complex hydraulic behavior, influencing flow patterns, velocity distribution and boundary shear stress distribution [9-11]. A critical factor affecting the hydraulic behavior of compound channels is energy dissipation [12]. The latter arises from turbulence generated at the boundaries, turbulence within the free shear layers, and velocity fluctuations associated with perturbations in the longitudinal secondary flow cells [13]. Notably, the previously unexplored horizontal shearing at the bank-full level in the main channel, occurring between the upper flow and the inbank flow, emerges as a significant source of energy loss in compound channels [12]. Furthermore, the distribution of turbulent kinetic energy at varying water depths and the variation of vertical turbulent kinetic energy can influence the dissipation rate of turbulent kinetic energy, thereby contributing to the overall energy dissipation process. These subtle aspects emphasize the necessity for a comprehensive understanding of the energy dissipation mechanisms in compound channels, which is crucial for the effective hydraulic modeling and management of water resources [13-16]. The VOF method, in conjunction with a turbulent model, is a valuable tool for analyzing hydraulic jumps. This study offers insights into the intricate dynamics of hydraulic jumps, particularly within the context of compound channels, and provides valuable information about the design and optimization of the hydraulic structures.

II. MATERIALS AND METHODS

A. Numerical Model

The present study uses ANSYS-FLUENT 17.2 to numerically examine the hydraulic jump in a compound channel from various openings, employing the VOF method of multi-phase flow theory. The geometry was created deploying the ANSYS software, and the meshing was completed utilizing the ANSYS Meshing, as shown in Figure 1. The VOF method was employed to ascertain the location of the water surface and to simulate the turbulence modeling of the hydraulic jump, by implementing the RNG k-ε model.

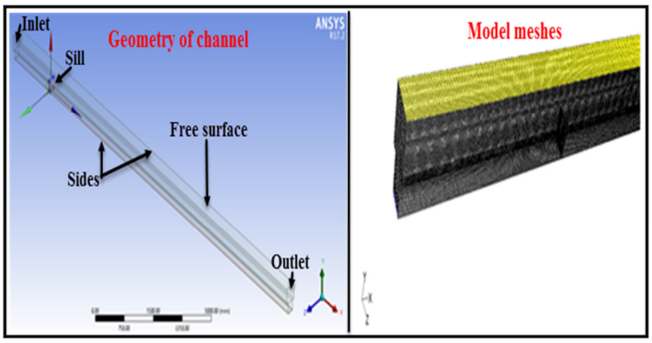

Fig. 1. Geometry and model meshes.

B. Boundary Conditions and Meshing

Table I provides a summary of the boundary conditions that have been imposed in the channel. In this analysis, two-phase water-air flows are considered, with the effect of air velocity being disregarded.

TABLE I. BOUNDARY CONDITIONS

Inlet	Outlet	Sides	Free surface	Sill
Inlet Velocity	Out flow	Wall	V=0	Wall

C. Theory

In this case study, the following mass conservation and momentum equations were applied to each fluid volume:

$$\frac{\partial \rho}{\partial t} + \sum_{j=1}^{3} \frac{\partial(\rho \bar{u}_i)}{\partial x_i} = 0 \quad (1)$$

The equations which are based on the assumptions of the unsteady, incompressible, and Newtonian flow, including the effect of gravity, can be expressed as follows:

$$\frac{\partial(\rho \overline{u_i})}{\partial t} + \sum_{j=1}^{3} \frac{\partial(\rho \overline{u_i u_j})}{\partial x_j} = -\frac{\partial p}{\partial x_i} + g_i + \sum_{j=1}^{3} \frac{\partial}{\partial x_j}\left[\mu\left(\frac{\partial \bar{u}_i}{\partial x_j} + \frac{\partial \bar{u}_j}{\partial x_i} - \frac{2}{3}\delta_{ij}\sum_{l=1}^{3}\frac{\partial \bar{u}_l}{\partial x_l}\right)\right] + \sum_{j=1}^{3}\frac{\partial}{\partial x_j}\left(-\rho\overline{u_i' u_j'}\right) + F_V \quad (2)$$

where, u is the velocity, t is the time, ρ is the fluid density, p is the pressure, v_t is the turbulent eddy-viscosity, g is the gravity acceleration and F_v is the body force. The Reynolds stress is:

$$-\rho\overline{u_i' u_j'} = \mu_t\left(\frac{\partial \bar{u}_i}{\partial x_j} + \frac{\partial \bar{u}_j}{\partial x_i}\right) - \frac{2}{3}\left(\rho k + \mu_t \sum_{l=1}^{3}\frac{\partial \bar{u}_l}{\partial x_l}\right)\delta_{ij} \quad (3)$$

where δ_{ij} is the Kronecker function. The Re- (RNG) methods followed to normalize the Navier-Stokes equations consider the impact of normalization groups at varying scales of motion, which contribute to turbulent diffusion. The RNG k-ε turbulence model is:

$$\frac{\partial(\rho k)}{\partial t} + \sum_{j=1}^{3}\frac{\partial(\rho k \bar{u}_j)}{\partial x_j} = \sum_{j=1}^{3}\frac{\partial}{\partial x_j}\left[\alpha_k \mu_{eff}\frac{\partial k}{\partial x_j}\right] + \bar{p}_k - \rho\varepsilon \quad (4)$$

$$\frac{\partial(\rho\varepsilon)}{\partial t} + \sum_{j=1}^{3}\frac{\partial(\rho\varepsilon \bar{u}_j)}{\partial x_j} = \sum_{j=1}^{3}\frac{\partial}{\partial x_j}\left[\alpha_\varepsilon \mu_{eff}\frac{\partial \varepsilon}{\partial x_j}\right] + C_{1\varepsilon}\frac{\varepsilon}{k}\bar{p}_k - C_{2\varepsilon}\rho\frac{\varepsilon^2}{k} - R_\varepsilon \quad (5)$$

$$\bar{p}_k = \sum_{i=1}^{3}\sum_{j=1}^{3}\left[\left(\mu_t\left(\frac{\partial \bar{u}_i}{\partial x_j} + \frac{\partial \bar{u}_j}{\partial x_i} - \delta_{ij}\sum_{l=1}^{3}\frac{2}{3}\frac{\partial \bar{u}_l}{\partial x_l}\right) - \frac{2}{3}\rho k \delta_{ij}\right)\frac{\partial \bar{u}_j}{\partial x_i}\right] \quad (6)$$

where μ_t is the viscosity:

$$\mu_t = \rho C_\mu \frac{k^2}{\varepsilon} \quad (7)$$

$$R_\varepsilon = \frac{C_\mu \rho \eta^3 (1-\eta/\eta_0)}{1+\beta\eta^3}\frac{\varepsilon^2}{k} \quad (8)$$

where $= \frac{sk}{\varepsilon}$, $\eta_0 = 4.38$, and $\beta = 0.012$. The constant values of the RNG k-ε model are:

$C_{1\varepsilon} = 1.42, C_{2\varepsilon} = 1.68, C_\mu = 0.0845\ \alpha_k = \alpha_\varepsilon \approx 1.393$.

D. Air–Water Two-Phase Flow Model

The VOF method [17], has been extensively employed in numerous research projects. In this method, the domain of computation is partitioned into discrete cells, or meshes. A discontinuous concentration function is assigned to each cell, representing the volume fraction of one of the cell's fluids. Subsequently, the position of the interface can be determined by means of an interface reconstruction procedure within each cell intersected by the interface, based on the information provided by the aforementioned cell fractions:

$$\rho = \alpha_l \rho_l + \alpha_a \rho_a \quad (9)$$

$$\mu = \alpha_l \mu_l + \alpha_a \mu_a \quad (10)$$

where the density (ρ) and dynamic viscosity (μ) of the mixture are functions of the volume fractions of each phase, and are calculated as:

$$\frac{\partial \alpha_l}{\partial t} + \sum_{j=1}^{3}\frac{\partial(\alpha_l \bar{u}_j)}{\partial x_j} = \frac{S_{M,l-a}}{\rho_l} \quad (11)$$

$$\frac{\partial \alpha_a}{\partial t} + \sum_{j=1}^{3}\frac{\partial(\alpha_a \bar{u}_j)}{\partial x_j} = \frac{S_{M,a-l}}{\rho_a} \quad (12)$$

E. Surface Tension

The Continuum Surface Force (CSF) model, as proposed by authors in [18], is employed in the computation of surface tension. In this model, the surface tension is regarded as a continuous function that considers three-dimensional effects across an interface rather than a boundary value condition. Consequently, the surface tension, σ, is a surface force that has been converted into a volume force, F_V, which acts as a source term in the momentum equation (2), and expressed as:

$$F_V = \sigma\frac{\alpha_l \rho_l K_a \nabla\alpha_a + \alpha_a \rho_a K_l \nabla\alpha_l}{\frac{1}{2}(\rho_l + \rho_a)} \quad (13)$$

where σ is the interfacial surface tension between a liquid and the surrounding air, K_l and K_a are the interface curvatures of the liquid, respectively. The surface tension coefficient, σ is equal to 0.07194 N/m at ambient temperature. The surface curvature, K, is defined in terms of the divergence of the unit normal, and the interface normal is determined through the evaluation of local gradients of volume fractions. The curvatures of the liquid are:

$$K_l = \frac{\Delta\alpha_l}{|\nabla\alpha_l|} \text{ and } K_a = \frac{\Delta\alpha_a}{|\nabla\alpha_a|} \quad (14)$$

The continuity equation (1) is used to track the interface between the phases, with air designated as the secondary phase and the interface is:

$$\frac{\partial(\alpha_2\rho_2)}{\partial t} + \frac{\partial(\alpha_2\rho_2 u_1)}{\partial x_i} = s_2 \quad (15)$$

where S_2 is the phase 2 source, ρ_2 is the air density and α_2 is the air volume fraction ($\alpha_2 = v_2/v$), where v is the fluid volume ($v = v_1 + v_2$) and v_1 and v_2 are, respectively, the volumes of phase 1 and phase 2. The volume fraction of the primary phase (water) is:

$$\sum_{i=1}^{2} a_i = 1 \quad (16)$$

III. EXPERIMENTAL WORK

The experimental studies were performed in a rectangular compound channel. The tests were held in a bench, as displayed in Figure 2, with a length of 10 m and a height of 0.5 m. The bench is surmounted by side walls made of transparent plexiglas with a thin sill in the form of a rectangular parallelepiped. The channel has a compound cross-section, a length of 10 m, a height of h = 20 cm, a width for the minor bed of b=15 cm, and a width for the major bed of b = 25 cm, as presented in Figure 3. The experimental study was carried out in a canal designed by the laboratory for the exploitation and development of natural resources in arid zones at the University of Ouargla.

Fig. 2. View of the channel.

Figure 4 depicts a sketch of the hydraulic jump parameters in a straight rectangular compound channel, where h_1 is the first consecutive depth, h_2 is the second consecutive depth, L_j is the length of jump, L_r is the length of roll, b is the width of main channel, and B is the width of floodplain.

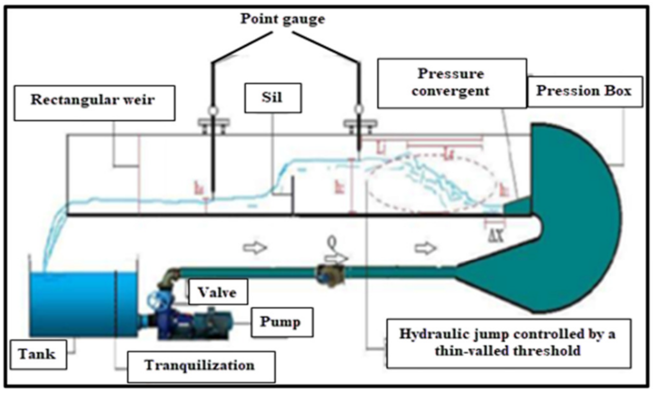

Fig. 3. General view of the channel.

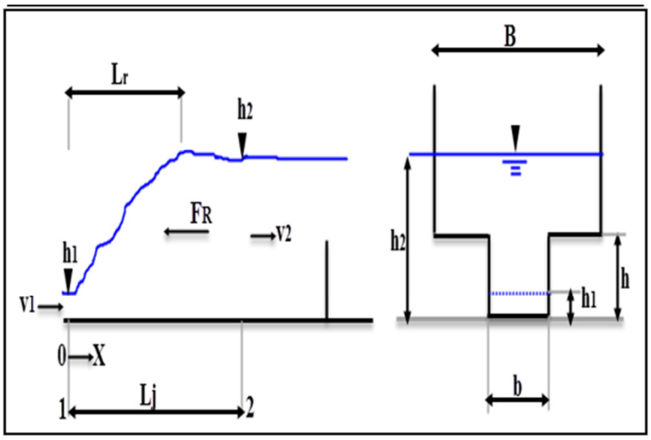

Fig. 4. Sketch of the hydraulic jump in a straight rectangular compound channel.

IV. RESULTS AND DISCUSION

In the present study, numerical simulations were performed to investigate the flow characteristics of a free-surface flow (hydraulic jump) in a straight composite rectangular channel with a weir [20]. The three-dimensional numerical results were obtained using the ANSYS FLUENT software, and employing the Reynolds-Averaged Navier-Stokes (RANS) turbulence model based on the RNG-k-ε approach. The free surface was determined by adopting the VOF method. The numerical model also demonstrated the formation and control of a hydraulic jump by a thin-wall weir, thereby underscoring the practical significance of the straight composite rectangular channel in terms of energy dissipation [21]. A hydraulic jump was generated with three distinct upstream section openings, designated as h_1 = 2 cm, 2.5 cm, and 4 cm, respectively. As the opening h_1 is increased, the hydraulic jump forms rapidly. The change in direction of the velocity vector fields before and after the hydraulic jump for each tested case is utilized to visualize the recirculation zone, hence providing insights into the flow dynamics and recirculation zones, as evidenced in Figure 5. Figure 6 presents the free surface profiles for different h_1 values, derived from both experimental observations and numerical simulations. Table II exhibits the dissipation rate results, with F_1 being the upstream Froude number, h_1 and h_2 the first and second sequent depth, Q the flow discharge, V_1 and

V_2 the upstream and downstream velocities, E_1 and E_2 the mean specific energy, η exp the experimental relative energy loss, η simul num the simulated relative energy loss and Err simul the simulated error.

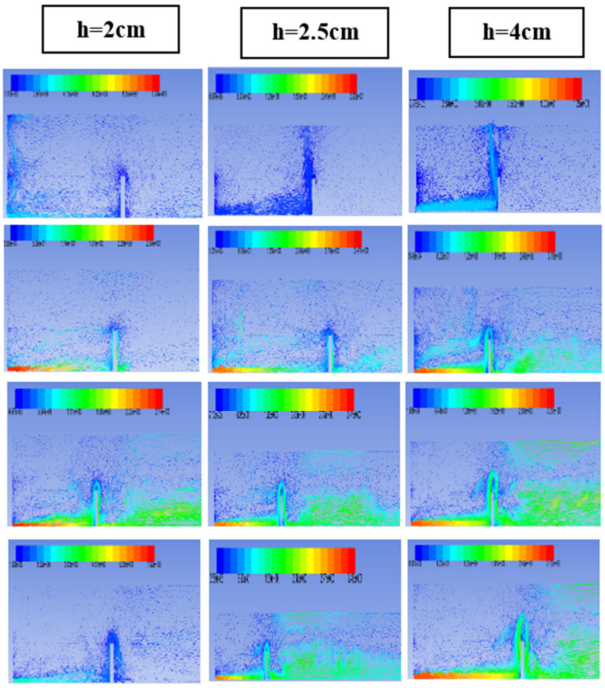

Fig. 5. The variation of the velocity vectors.

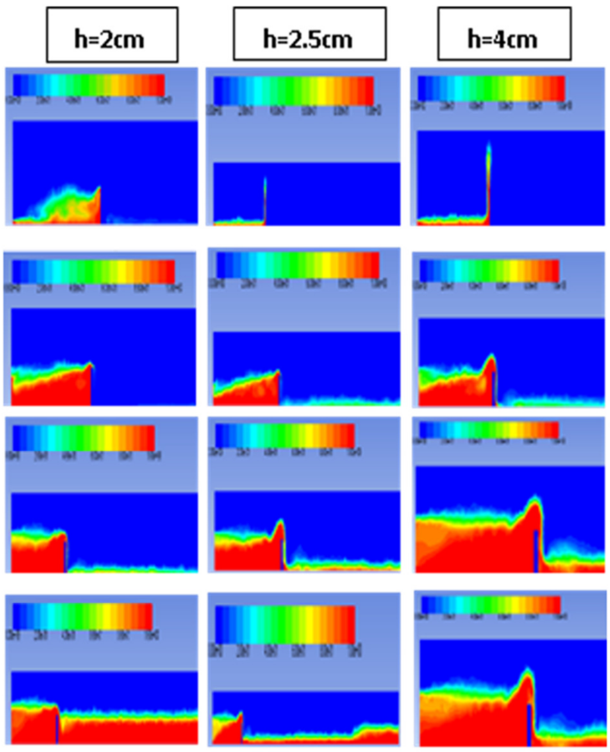

Fig. 6. The variation of the free surface.

TABLE II. DISSIPATION RATE EXPERIMENTAL AND NUMERICAL RESULTS

F_1	h_1 (m)	h_2 (m)	Q (m^3/s)	V_1 (m/s)	V_2 (m/s)
12	0.02	0.309	0.0155	5.17	0.93
9	0.025	0.295	0.0169	4.51	1.02
6	0.04	0.322	0.02373	3.96	1.05

E_1 (m)	E_2 (m)	η exp (%)	η simul. num. (%)	Err. simul. (%)
1.3806	0.3531	77.47	74.42	3.9
1.0602	0.3480	71.90	67.17	6.6
0.8372	0.3782	60.53	54.83	9.4

A reduction in efficiency was proven to be associated with an increase in the opening parameter, h1, in the VOF turbulent model analysis of hydraulic jumps. The model is found to be an accurate and reliable tool for modeling hydraulic jumps, with an error of less than 10% compared to the experimental results. This quantitative evaluation highlights the model's ability to capture the complex nature of practical hydraulic conditions. The results provide evidence of the usefulness of the numerical approach in real-world scenarios and offer insights into the hydraulic jump behavior. Overall, the VOF turbulent model is a reliable resource for understanding and modeling hydraulic processes.

V. CONCLUSIONS

This study analyzed hydraulic jumps in a compound channel through the use of both experimental and numerical methods. The RNG k-ε turbulence model with the Volume of Fluid (VOF) method was found to accurately simulate the experimental observations. The study's key findings include insights into the influence of upstream openings on jump formation and energy dissipation efficiency. The numerical model, validated by experimental results, represents a cost-effective tool for the analysis of the hydraulic jumps in compound channels. The findings of this research offer valuable insights that can inform the design and optimization of hydraulic structures:

- The numerical and experimental results, when considered across the three opening scenarios, serve to validate the adopted numerical model. Furthermore, they demonstrate a high degree of coherence in terms of energy dissipation efficiency.
- The numerical model provides a clear representation of the longitudinal and transverse evolution of the hydraulic jump in the rectangular compound channel.
- The numerical model adopted in this study can serve as a cost-effective alternative to experimental manipulations in cases where constructing a reduced-scale model is challenging.

REFERENCES

[1] K. Laishram, T. Devi, N. Singh, and P. Kumar, "Numerical and Experimental Study on Energy Dissipation in Hydraulic Jump: A Comparison Between Horizontal and Sloping Rough Channel Bed," in *9th IAHR International Symposium on Hydraulic Structures (9th ISHS)*, Roorkee, India, Oct. 2022, https://doi.org/10.26077/cb4c-fdc3.

[2] H. Chanson, Ed., *Energy Dissipation in Hydraulic Structures*, 1st ed. London, UK: CRC Press, 2015.

[3] A. S. Ramamurthy, J. Qu, and D. Vo, "Numerical and Experimental Study of Dividing Open-Channel Flows," *Journal of Hydraulic Engineering*, vol. 133, no. 10, pp. 1135–1144, Oct. 2007, https://doi.org/10.1061/(ASCE)0733-9429(2007)133:10(1135).

[4] J. J. Rebollo, D. López, L. Garrote, T. Ramos, R. Díaz, and R. Herrero, "Experimental Analysis of the Influence of Aeration in the Energy Dissipation of Supercritical Channel Flows," *Water*, vol. 11, no. 3, Mar. 2019, Art. no. 576, https://doi.org/10.3390/w11030576.

[5] A. N. AlTalib, A. Y. Mohammed, and H. A. Hayawi, "Hydraulic jump and energy dissipation downstream stepped weir," *Flow Measurement and Instrumentation*, vol. 69, Oct. 2019, Art. no. 101616, https://doi.org/10.1016/j.flowmeasinst.2019.101616.

[6] M. H. Jafari Abnavi, R. Mohammadpour, and M. K. Beirami, "Laboratory investigation of hydraulic jump in divergent-convergent conversions," *Flow Measurement and Instrumentation*, vol. 94, Dec. 2023, Art. no. 102444, https://doi.org/10.1016/j.flowmeasinst.2023.102444.

[7] P. K. Singh, X. Tang, and H. Rahimi, "Large-Eddy Simulation of Compound Channels with Staged Floodplains: Flow Interactions and Turbulent Structures," *Water*, vol. 15, no. 5, Jan. 2023, Art. no. 983, https://doi.org/10.3390/w15050983.

[8] V. T. Chow, *Open Channel Hydraulics*. Blackburn Press, 2009.

[9] S. C. A. Elliott and R. H. J. Sellin, "SERC flood channel facility: skewed flow experiments," *Journal of Hydraulic Research*, vol. 28, no. 2, pp. 197–214, Mar. 1990, https://doi.org/10.1080/00221689009499086.

[10] D. Bousmar, N. Wilkin, J.-H. Jacquemart, and Y. Zech, "Overbank Flow in Symmetrically Narrowing Floodplains," *Journal of Hydraulic Engineering*, vol. 130, no. 4, pp. 305–312, Apr. 2004, https://doi.org/10.1061/(ASCE)0733-9429(2004)130:4(305).

[11] B. Rezaei and D. W. Knight, "Overbank Flow in Compound Channels with Nonprismatic Floodplains," *Journal of Hydraulic Engineering*, vol. 137, no. 8, pp. 815–824, Aug. 2011, https://doi.org/10.1061/(ASCE)HY.1943-7900.0000368.

[12] S. Proust, D. Bousmar, N. Rivière, A. Paquier, and Y. Zech, "Energy losses in compound open channels," *Advances in Water Resources*, vol. 33, no. 1, pp. 1–16, Jan. 2010, https://doi.org/10.1016/j.advwatres.2009.10.003.

[13] K. Shiono and D. W. Knight, "Turbulent open-channel flows with variable depth across the channel," *Journal of Fluid Mechanics*, vol. 222, pp. 617–646, Jan. 1991, https://doi.org/10.1017/S0022112091001246.

[14] A. Kozioł, "Turbulent kinetic energy of water in a compound channel," *Annals of Warsaw University of Life Sciences - SGGW. Land Reclamation*, vol. 43, no. 2, pp. 193–205, Jan. 2011, https://doi.org/10.2478/v10060-011-0055-z.

[15] B. G. Krishnappan and Y. L. Lau, "Turbulence Modeling of Flood Plain Flows," *Journal of Hydraulic Engineering*, vol. 112, no. 4, pp. 251–266, Apr. 1986, https://doi.org/10.1061/(ASCE)0733-9429(1986)112:4(251).

[16] P. Ackers, *Hydraulic design of straight compound channels. Volume 1 - summary and design method, Volume 2 - appendices*, UK: HR Wallingford, 1991.

[17] C. W. Hirt and B. D. Nichols, "Volume of fluid (VOF) method for the dynamics of free boundaries," *Journal of Computational Physics*, vol. 39, no. 1, pp. 201–225, Jan. 1981, https://doi.org/10.1016/0021-9991(81)90145-5.

[18] J. U. Brackbill, D. B. Kothe, and C. Zemach, "A continuum method for modeling surface tension," *Journal of Computational Physics*, vol. 100, no. 2, pp. 335–354, Jun. 1992, https://doi.org/10.1016/0021-9991(92)90240-Y.

[19] W. Djam and A. Ghomri, "Study of the experimental approach of the relative length of the surface role of the hydraulic jump evolving in rectangular channel of section composed with rough bottom," *Journal of Fundamental and Applied Sciences*, vol. 12, no. 3, pp. 1190–1203, Sep. 2020, https://doi.org/10.4314/jfas.v12i3.13.

[20] M. Alsaydalani, "Hydraulic Jump Characteristics Downstream of a Compound Weir consisting of Two Rectangles with a below Semicircular Gate," *Engineering, Technology & Applied Science Research*, vol. 14, no. 2, pp. 13266–13273, Apr. 2024, https://doi.org/10.48084/etasr.6918.

[21] F. Rooniyan, "The Effect of Confluence Angle on the Flow Pattern at a Rectangular Open-Channel," *Engineering, Technology & Applied Science Research*, vol. 4, no. 1, pp. 576–580, Feb. 2014, https://doi.org/10.48084/etasr.395.